

DEPHASING PARAMETERS (TIME, DECREMENT, AND ANGLE) AND THEIR DEPENDENCE ON PRESSURE; DEPHASING DECELERATION AND ACCELERATION EFFECTS

Yu. E. D'yakov

A detailed mathematical description is developed for the dephasing time τ_{ph} as a function of pressure in different particle velocity correlation models. New polarization damping parameters (the dephasing decrement m_{ph} and angle φ) are introduced and their dependence on pressure is considered. The thresholds of the appearance of characteristic extrema (the Dicke dip, the peak of the function τ_{ph} , etc.) are calculated for different substances. A "spectron" method is suggested for measuring the polarization damping spectrum using a single laser shot.

1. The dependence of the spectral width $\Delta\omega$ on a pressure p , which is due to the Doppler and collisional dephasing mechanisms, for some media can be represented as a monotonically increasing curve. For other media the value of $\Delta\omega$ first decreases with increasing p (the Dicke narrowing), passes through a minimum (the Dicke dip), and then increases (Fig. 1 a; see, e. g., [1, p. 18] and [2, p. 89]). In this case the estimate for $\Delta\omega$ is determined from a certain level $1 - \varepsilon$ above the spectrum base (Fig. 1 b) measured by methods of stationary spectroscopy; usually $\varepsilon = 0.5$ is taken.

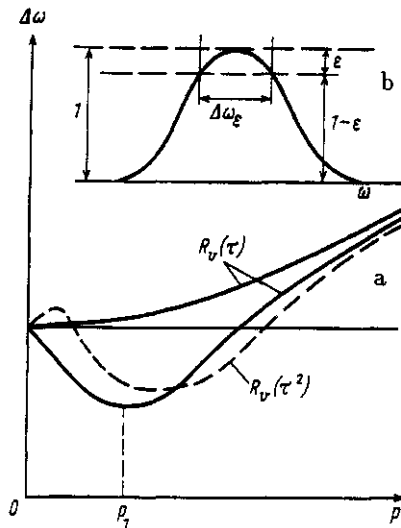


Fig. 1

In the nonstationary spectroscopy a process developing in time is observed, namely the damping of the intensity $\mathcal{J}(t)$ of molecular oscillations excited by a sufficiently short initial field pulse (Fig. 2). The rate of the drop of the curve $\mathcal{J}(t)$ characterizes the dephasing rate. This can be estimated quantitatively by introducing the dephasing time τ_{ph} corresponding to the e^{-2m} -fold ($m > 0$) \mathcal{J} drop [3]. The question of τ_{ph} dependence on p was investigated in [3] (see also [4, 5]).

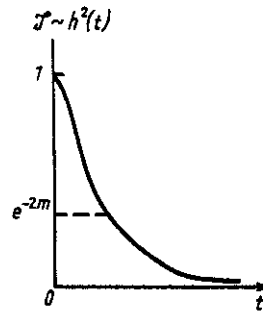


Fig. 2

Unlike $\Delta\omega(p)$, the function $\tau_{ph}(p)$ can have different forms even for one and the same substance depending on the chosen value of m (Fig. 3). For $m < m_0$ (m_0 is a substance parameter not dependent on pressure; see below) the magnitude of τ_{ph} decreases monotonically with increasing p . Hence, in this case the dephasing is accelerated in the passage to higher pressures because less time is required to attain the level e^{-2m} . In the case $m > m_0$ we first have an interval of τ_{ph} growth (the dephasing *deceleration* interval $0 < p < p_1$), and then the function $\tau_{ph}(p)$ passes through a maximum and subsequently decreases (the dephasing *acceleration* interval $p > p_1$; see Fig. 3).

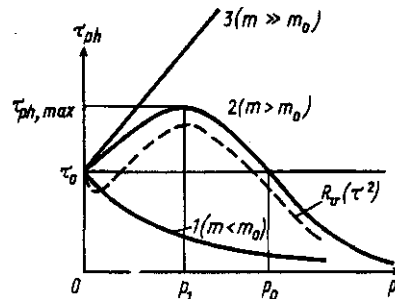


Fig. 3

This pattern is observed when two dephasing mechanisms are taken into account, namely the Doppler mechanism (dominating on deceleration intervals) and the collisional mechanism (dominating on acceleration intervals).

2. To describe the damping of the intensity $J(t) = J(0)h^2(t)$ of molecular oscillations the expression

$$h(t) = e^{-L(t)}, \quad L(t) = \frac{t}{T_c} + k_0^2 \int_0^t (t - \tau) B_v(\tau) d\tau \quad (1)$$

was obtained [3-5].

The first term in (1) describes the collisional dephasing, and the other term describes the Doppler dephasing; T_c is the relaxation time relating to the variation of the radiation frequency during collisions; $k_0 = \omega_0/c$ is the wave number of molecular oscillations; $B_v(\tau) = \langle v_z v_{z,\tau} \rangle = \sigma_v^2 R(\tau/\tau_v)$ is the particle velocity correlation function in the wave propagation direction z , $\sigma_v^2 = kT/\mu$ (k is Boltzmann's constant, T is temperature, and μ is the particle mass), $R(\tau/\tau_v)$ is the thermal velocity correlation coefficient; and the

corresponding correlation time τ_v is defined by the relation

$$\tau_v = \int_0^{\infty} R(\tau/\tau_v) d\tau \quad \text{or} \quad \int_0^{\infty} R(x) dx = 1. \quad (2)$$

Based on (1), an explanation was for the first time given [3, 4] to the experimentally observed damping of molecular oscillations in gases according to a nonlinear exponential law, which for large and small t goes into a linear law:

$$h(t \rightarrow 0) = \exp\left\{-\frac{t}{T_c} - \frac{1}{2}\nu_0^2 t^2\right\}, \quad h(t \rightarrow \infty) = \exp\left\{-\frac{t}{T_2} + \nu_0^2 \tau_v^2 y_1\right\} \\ \left(\nu_0 = k_0 \sigma_v, \quad \frac{1}{T_2} = \frac{1}{T_c} + \nu_0^2 \tau_v, \quad y_1 = \int_0^{\infty} x R(x) dx\right). \quad (3)$$

In what follows we assume that

$$\frac{1}{T_c} = \alpha p, \quad \frac{1}{\tau_v} = \beta p, \quad \left(\gamma = \frac{\beta}{\alpha} = \frac{T_c}{\tau_v} = \text{const}\right), \quad (4)$$

where $\alpha, \beta > 0$. Expression (1) can be rewritten in the form

$$L(t) = y/\gamma + \nu_0^2 t^2 F(y)y^{-2} = y/\gamma + (\nu_0/\beta p)^2 F(y), \\ (y = t/\tau_v = \beta p t), \quad (5)$$

where

$$F(y) = \int_0^y (y-x)R(x) dx, \quad F(y) = \frac{1}{2}y^2 \quad (y \rightarrow 0), \quad y - y_1 \quad (y \rightarrow \infty). \quad (6)$$

If we now represent $R(x)$ as an expansion

$$R(x) = \sum_{n=0}^{\infty} R_n x^n \quad (R_0 = 1, R_1 \leq 0), \quad (7)$$

this results in

$$F(y) = y^2 \sum_{n=0}^{\infty} \frac{R_n y^n}{(n+1)(n+2)}, \\ L(t) = \alpha p t + \nu_0^2 t^2 \sum_{n=0}^{\infty} \frac{R_n}{(n+1)(n+2)} (\beta p t)^n. \quad (8)$$

3. In the discussion of the results of [3] it was suggested that the case of small ε for the function $\Delta\omega_\varepsilon(p)$ was a complete analog of the case of large m for $\tau_{ph}(p)$ so that reducing ε (i.e., measuring the width of only the apex of the spectrum) it is possible to produce the appearance of the Dicke dip for any medium. We shall show that this is not the case [6]. Denote by $\Delta\omega_\varepsilon$ the width of the apex of the spectrum

$G(\omega) = \int_0^{\infty} h(t) \cos \omega t dt$ ($\varepsilon \ll 1$; see Fig. 1 b). It is clear that with decreasing ε the magnitude of $\Delta\omega_\varepsilon$ also decreases, and it can be estimated using the expansion

$$G(\omega) \approx G(0) - \frac{1}{2}\omega^2 \left| \frac{\partial^2 G}{\partial \omega^2} \right|_{\omega=0}.$$

Setting $\omega = (1/2)\Delta\omega_\varepsilon$ and $G(\omega)/G(0) = 1 - \varepsilon$ here, we obtain

$$\Delta\omega_\varepsilon = \sqrt{8\varepsilon/\langle\tau^2\rangle}, \quad \langle\tau^2\rangle = \int_0^\infty h(t)t^2 dt / \int_0^\infty h(t) dt. \quad (9)$$

In (9) only the parameter $\langle\tau^2\rangle$ unrelated to ε may depend on p . Hence, p and ε affect $\Delta\omega_\varepsilon$ independently, i.e., the variation of ε produces no effect on the appearance or disappearance of the Dicke dip. As is shown below, the threshold of the appearance of the Dicke dip for $\Delta\omega_\varepsilon$ turns out to be even *higher* than for the quantity $\Delta\omega$ determined from the level $\varepsilon \approx 0.5$ (see Section 8).

4. According to (1), the dephasing time τ_{ph} is determined by the relation

$$L(\tau_{ph}) = m. \quad (10)$$

Using Eq. (5) we can represent Eq. (10) as

$$y/\gamma + \nu_0^2 \tau_{ph}^2 F(y) y^{-2} = m \quad (y = \tau_{ph}/\tau_v = \beta p \tau_{ph}), \quad (11)$$

that is

$$y/\gamma + \left(\frac{\nu_0}{\beta p}\right)^2 F(y) = m. \quad (12)$$

It follows that

$$\tau_{ph}(y) = \frac{y}{\nu_0} \sqrt{\frac{m - y/\gamma}{F(y)}}, \quad p(y) = \frac{\nu_0}{\beta} \sqrt{\frac{F(y)}{m - y/\gamma}}. \quad (13)$$

As is implied by (13), for $0 < p < \infty$ the magnitude of y varies within the limits

$$0 < y < y_{\max}, \quad y_{\max} = m\gamma. \quad (14)$$

By virtue of (8), we rewrite (11) in the form

$$\alpha p \tau_{ph} + \nu_0^2 \tau_{ph}^2 \sum_{n=0}^{\infty} \frac{R_n}{(n+1)(n+2)} (\beta p \tau_{ph})^n = m. \quad (15)$$

According to (15), up to within the terms of the first order with respect to p (i.e., in the interval of low pressures) we have

$$\tau_{ph}(p) = \tau_0 + \tau'_0 p, \quad (16)$$

where

$$\tau_0 = \frac{\sqrt{2m}}{\nu_0}, \quad \tau'_0 = \frac{\alpha}{\nu_0^2} (M - 1), \quad M = \frac{m|R_1|}{3} \gamma \equiv \frac{m}{m_0}, \quad m_0 = \frac{3}{\gamma|R_1|}. \quad (17)$$

To the curves of types 2 and 3 in Fig. 3 there corresponds $\tau'_0 > 0$, or, according to (17),

$$\gamma > \frac{3}{m|R_1|} \quad (\text{or } m > m_0, M > 1). \quad (18)$$

In the opposite limiting case of high pressures we have, according to (8) and (12),

$$y \rightarrow y_\infty = \beta p \tau_{ph} \approx m, \quad \tau_{ph} \approx \frac{m}{\alpha p} = mT_c. \quad (19)$$

5. We consider some special correlation models for thermal particle velocities.

1) An analytical expression for $\tau_{ph}(p)$ applicable for all p can be obtained in the case $\beta = 0$ when only the collisional dephasing acts while the Doppler dephasing is negligibly small. In this case $\tau_v = \infty$, $\gamma = 0$, $m_0 = \infty$, $M = 0$, $y = 0$,

$$R(x) = 1, \quad F(x) = (1/2)x^2, \quad (20)$$

and Eq. (7) assumes the form

$$\alpha p \tau_{\text{ph}} + (1/2) \nu_0^2 \tau_{\text{ph}}^2 = m,$$

whence

$$\tau_{\text{ph}}(p) = \frac{\alpha p}{\nu_0^2} \left(\sqrt{1 + 2m \left(\frac{\nu_0}{\alpha p} \right)^2} - 1 \right). \quad (21)$$

Formula (21) agrees with the earlier asymptotic estimates (16) and (19). Curve 1 in Fig. 3 corresponds to (21).

2) The explicit form of the function $\tau_{\text{ph}}(p)$ can also be found if we assume that [6]

$$R(x) = \frac{1}{(1+x/2)^3}, \quad F(x) = \frac{x^2}{2+x}, \quad R_1 = -3/2. \quad (22)$$

In this case $M = m\gamma/2$, $m_0 = 2/\gamma$, $y_{\text{max}} = 2M$, and Eq. (12) takes the form

$$y + \frac{\lambda y^2}{2+y} = m\gamma \quad \left(\lambda = \frac{\nu_0^2}{\alpha \beta p^2} \right)$$

and is transformed into the quadratic equation

$$(1+\lambda)y^2 + (2-m\gamma)y - 2m\gamma = 0, \quad (23)$$

from which we find

$$y = \frac{m\gamma/2 - 1}{1+\lambda} \pm \sqrt{\left(\frac{m\gamma/2 - 1}{1+\lambda} \right)^2 + \frac{2m\gamma}{1+\lambda}} > 0,$$

that is

$$\tau_{\text{ph}}(p) = \frac{m\gamma/2 - 1}{\beta p (1 + \nu_0^2 / \alpha \beta p^2)} \left[1 \pm \sqrt{1 + 2m\gamma \frac{1 + \nu_0^2 / \alpha \beta p^2}{(m\gamma/2 - 1)^2}} \right] > 0. \quad (24)$$

According to (24), for a purely Doppler dephasing ($\alpha = 0$ and $T_c = \infty$) the function $\tau_{\text{ph}}(p)$ is monotonically increasing:

$$\tau_{\text{ph}}(p)_{\alpha=0} = \frac{m\beta p}{2\nu_0^2} \left[1 + \sqrt{1 + \frac{8\nu_0^2}{mp^2\beta^2}} \right] \quad (25)$$

(Fig. 3, curve 3), and for a purely collisional dephasing ($\beta = 0$ and $\tau_v = \infty$) it is monotonically decreasing:

$$\tau_{\text{ph}}(p)_{\beta=0} = \frac{\alpha p}{2\nu_0^2} \left(\sqrt{1 + 8m \left(\frac{\nu_0}{\alpha p} \right)^2} - 1 \right) \quad (26)$$

as in model (20), but according to a different law (Fig. 3, curve 1; cf. (21) and (26)). We find the "width" p_0 of the peak of τ_{ph} (see Fig. 3) by setting $\tau_{\text{ph}} = \tau_0 = \sqrt{2m}/\nu_0$ in (24). This results in

$$\begin{aligned} p_0 &= \frac{2}{\beta \tau_0} (M - 1) = \left(\sqrt{M} + \frac{1}{\sqrt{M}} \right) \frac{\nu_0}{\sqrt{\alpha \beta}}, \\ y_0 &= \beta p_0 \tau_0 = 2(M - 1) = y_{\text{max}} - 2. \end{aligned} \quad (27)$$

To find the point on the curve $\tau_{\text{ph}}(p)$ where $\tau_{\text{ph}} = \tau_{\text{ph,max}}$ and $p = p_1$ we can test function (24) for maximum. In the case under consideration one can apply a different technique because it is easy to find the inverse function

$$p(\tau_{\text{ph}}) = \frac{M - 1}{\beta \tau_{\text{ph}}} \pm \sqrt{\left(\frac{M - 1}{\beta \tau_{\text{ph}}} \right)^2 - \frac{\nu_0^2 (\tau_{\text{ph}}^2 - \tau_0^2)}{\alpha \beta \tau_{\text{ph}}^2}} \quad (28)$$

from (23). The two pressure values determined by formula (28) must obviously coincide at $p = p_1$. Therefore, equating the root in (28) to zero we obtain

$$\tau_{\text{ph, max}} (= \tau_1) = \frac{M+1}{\nu_0 \sqrt{\gamma}}, \quad p_1 = \frac{M-1}{M+1} \frac{\nu_0}{\sqrt{\alpha\beta}} = \frac{M-1}{M+1} \frac{\nu_0 \sqrt{\gamma}}{\beta}. \quad (29)$$

For the relative maximum formula (29) yields

$$\kappa = \tau_{\text{ph, max}} / \tau_0 = \frac{1}{2} \left(\sqrt{M} + \frac{1}{\sqrt{M}} \right), \quad M = (\kappa + \sqrt{\kappa^2 - 1})^2. \quad (30)$$

3) The model

$$R(x) = e^{-x}, \quad F(x) = x - 1 + e^{-x}, \quad R_1 = -1 \quad (31)$$

is frequently used in spectroscopic calculations [4, 7]. In [4] the conclusion was drawn that the experimental data obtained by the method of nonstationary (picosecond) active spectroscopy corresponded to model (31) best of all.

4) The case

$$R(x) = (1+x^2)^{-\frac{3}{2}}, \quad F(x) = \sqrt{1+x^2} - 1, \quad R_1 = 0, \quad R_2 = -\frac{3}{2} \quad (32)$$

fundamentally differs from (22), (20), and (31) in that R depends not on x but on x^2 and $R_1 = 0$ in expansion (13), i.e., the above criterion (18) for the appearance of maximum on the curve $\tau_{\text{ph}}(p)$ is inapplicable here. Below this question is considered in more detail (Section 9). We note that model (32) agrees well with the experimental values of τ_{ph} for hydrogen (see [5, Figs. 5 and 4]).

The substitution of (32) into (12) results in the equation

$$y/\gamma + \lambda(\sqrt{1+y^2} - 1) = m, \quad \lambda = (\nu_0/\beta p)^2, \quad y = \beta p \tau_{\text{ph}},$$

which is reduced to the quadratic equation

$$(\lambda^2 \gamma^2 - 1)u^2 + 2(\lambda + m)u - m(2\lambda + m) = 0 \quad (u = y/\gamma = \alpha p \tau_{\text{ph}}),$$

whence

$$\begin{aligned} \tau_{\text{ph}} &= \frac{1}{\alpha p} \left[\sqrt{\left(\frac{\lambda + m}{\lambda^2 \gamma^2 - 1} \right)^2 + \frac{m(2\lambda + m)}{\lambda^2 \gamma^2 - 1}} - \frac{\lambda + m}{\lambda^2 \gamma^2 - 1} \right] \quad \left(\lambda \gamma > 1, p < \frac{\nu_0}{\sqrt{\alpha\beta}} \right), \\ &= \frac{m\sqrt{\gamma}}{2\nu_0} \frac{2 + m\gamma}{1 + m\gamma} \quad \left(\lambda \gamma = 1, p = \frac{\nu_0}{\sqrt{\alpha\beta}} \right), \\ &= \frac{1}{\alpha p} \left[\frac{\lambda + m}{1 - \lambda^2 \gamma^2} - \sqrt{\left(\frac{\lambda + m}{\lambda^2 \gamma^2 - 1} \right)^2 - \frac{m(2\lambda + m)}{1 - \lambda^2 \gamma^2}} \right] \quad \left(\lambda \gamma < 1, p > \frac{\nu_0}{\sqrt{\alpha\beta}} \right). \end{aligned}$$

6. We consider some versions of the construction of the curve $\tau_{\text{ph}}(p)$ using the formulas in Section 4 which determine the function $\tau_{\text{ph}}(p)$ only in *implicit* form.

1) Let the function $R(x)$ and the parameters α , β , ν_0 , and m be given. We first find the function $F(y)$ determined by integral (6). Then for an arbitrary value of y_i belonging to interval (14) we determine $\tau_{\text{ph}, i} = \tau_{\text{ph}}(y_i)$ and $p_i = y_i/\beta\tau_{\text{ph}, i}$ by formula (13). The curve $\tau_{\text{ph}}(p)$ is constructed from the resulting points $\tau_{\text{ph}, i}$ and p_i .

2) Let the initial conditions be the same. Again, setting the values of y_i we find p_i from formula (13) and then determine $\tau_i = y_i/\beta p_i$.

3) The parameters α , β , and ν_0 are unknown, and the curve $\tau_{\text{ph}}(p)$ corresponding to the given value of m is constructed from experimental points and has a maximum $\tau_{\text{ph, max}}$ at p_1 .

Thus, from τ_0 and m we find the first estimate $\nu_0 = \sqrt{2m}/\tau_0$. After that, on choosing a certain model for the correlation coefficient $R(x)$ and determining the corresponding function $F(y)$, we construct the curves (13)

$$\tau_{\text{ph}}(y) = \frac{y}{\nu_0} \sqrt{\frac{m - y/\gamma}{F(y)}} \quad (33)$$

for different values of γ so that $\tau_{\text{ph}, \text{max}}$ coincides with the known experimental value. Here we essentially use the fact that the function $\tau_{\text{ph}}(p)$ possesses maximum, the value of this peak not depending on whether τ_{ph} is regarded as a function of p or y . Let the coincidence be attained for some γ and y . This makes it possible to find estimates for the parameters α and β : $\beta = y/(p\tau_{\text{ph}, \text{max}})$ and $\alpha = \beta/\gamma$. Furthermore, we use these estimates to construct the curve $\tau_{\text{ph}}(p)$ by points according to the above versions 1 or 2. If the resulting curve τ_{ph} differs from the experimental curve, the calculation can be repeated for another model of $R(x)$.

We note that when constructing curves (33) one can use the estimate for γ following from model (22) as a tentative result. Namely, on estimating the "contrast" $\kappa = \tau_{\text{ph}, \text{max}}/\tau_0$ from the experimental curve we find

$$M = (\kappa + \sqrt{\kappa^2 - 1})^2, \quad \gamma = \frac{2M}{m}$$

(see (17) and (30)).

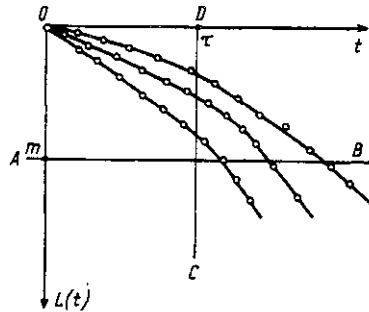


Fig. 4

7. We introduce the *dephasing decrement* m_{ph} defined as the polarization damping coefficient for a fixed time τ . According to (1), we have

$$m_{\text{ph}} = L(\tau) = \frac{\tau}{T_c} + k_0^2 \int_0^\tau (\tau - \tau') B_v(\tau') d\tau'. \quad (34)$$

The dependence of m_{ph} on p is found from the points of intersection of the curves $L(\tau)$ with the vertical line CD; recall that the dependence of τ_{ph} on p was determined from the points of intersection of the same curves with the horizontal line AB (Fig. 4). The two functions τ_{ph} and m_{ph} depend on the same parameters (α , β , ν_0), that is, in the spectroscopic aspect they are equally informative. However, the function m_{ph} is more convenient for estimating these parameters because its form is known. Indeed, according to (34) and (7), we have

$$m_{\text{ph}}(p) = u/\gamma + 2m_{\text{ph}, 0} F(u) u^{-2} = u/\gamma + 2m_{\text{ph}, 0} \sum_{n=0}^{\infty} \frac{R_n u^n}{(n+1)(n+2)}, \quad (35)$$

$$\left(u = \beta p \tau, \quad m_{\text{ph}, 0} = m_{\text{ph}}(p=0) = \frac{1}{2} \nu_0^2 \tau^2 \right). \quad (36)$$

Sometimes it is more convenient to write expression (35) in the form

$$n_{ph}(p) = u + 2n_0 F(u)u^{-2} = u + 2n_0 \sum_{n=0}^{\infty} \frac{R_n u^n}{(n+1)(n+2)}, \quad (37)$$

$$(n_0 = \gamma m_{ph,0}), \quad (38)$$

using the normalized dephasing decrement $n_{ph}(p) = \gamma m_{ph}(p)$. In particular, for high and low pressures we have

$$m_{ph}(p) = m_{ph,0} - (N^2 - 1)u/\gamma (p \rightarrow 0); \quad u/\gamma = \tau/T_c (p \rightarrow \infty), \quad (39)$$

where

$$N = \frac{\tau}{\tau_{th}} = \tau \nu_0 \sqrt{\frac{1}{6} |R_1| \gamma}, \quad \tau_{th} = \frac{1}{\nu_0} \sqrt{\frac{6}{|R_1| \gamma}}. \quad (40)$$

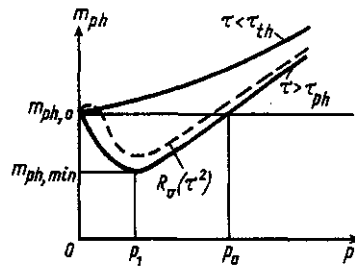


Fig. 5

The graph of the function $m_{ph}(p)$ resembles that of $\Delta\omega(p)$, namely the magnitude of m_{ph} either increases with increasing p or first decreases, passes through a minimum (analogous to the Dicke dip) and then increases (Fig. 5). However, it is important that, in contrast to $\Delta\omega$, the function $m_{ph}(p)$ with a dip can be obtained for any substance by taking a sufficiently long delay τ :

$$\tau > \tau_{th}, \quad \text{that is} \quad \gamma > \frac{6}{|R_1|(\nu_0 \tau)^2}. \quad (41)$$

Example. In the case of model (22) we have

$$n_{ph}(p) = u + \frac{4N^2}{2+u} \quad \left(u = \beta p \tau, \quad N = \frac{1}{2} \tau \nu_0 \sqrt{\gamma} \right). \quad (42)$$

The minimum of function (42) is at $u_1 = 2(N-1)$, i.e., it corresponds to the pressure p_1 :

$$p_1 = \frac{2(N-1)}{\beta \tau}, \quad n_{ph,min} = 2(2N-1). \quad (43)$$

The "dip" width at the level $n_{ph,0}$ is $p_0 = 2(N^2 - 1)/\beta \tau = (N+1)p_1$. We note that, according to (42) and (43), for sufficiently large τ , i.e., for $N \gg 1$ or $(1/2)\tau \nu_0 \sqrt{\gamma} \gg 1$ or $\gamma \gg (2/\tau \nu_0)^2$, the pressure p_1 corresponding to $n_{ph,min}$ no longer depends on τ :

$$p_1 = \frac{2}{\beta \tau} \left(\frac{1}{2} \tau \nu_0 \sqrt{\gamma} - 1 \right) \rightarrow \frac{\nu_0}{\sqrt{\alpha \beta}}.$$

It is easy to show that for $m \gg m_0$ the maximum of the dephasing time τ_{ph} also corresponds to the same pressure $\nu_0/\sqrt{\alpha \beta}$.

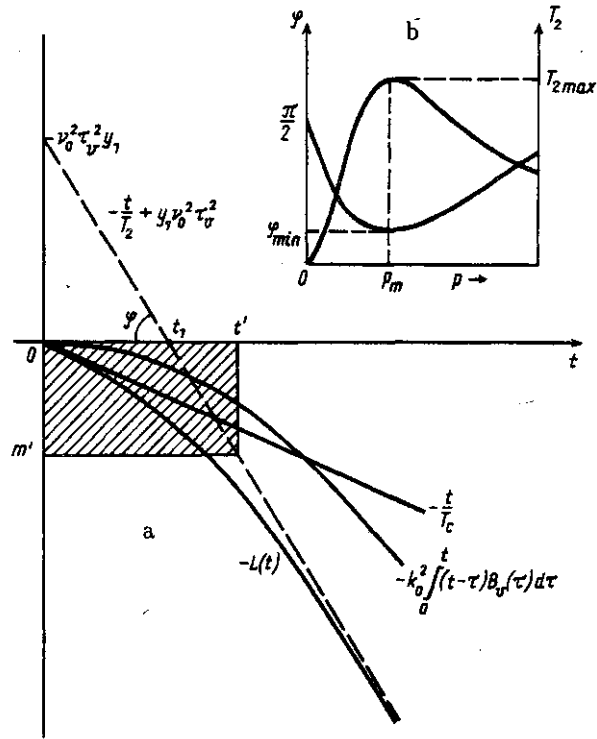


Fig. 6

We can also introduce the *dephasing angle* φ determining the slope of the line $-t/T_2 + \nu_0^2 \tau_v^2 y_1$ with respect to the axis $\nu_0 t$ (Fig. 6 a):

$$\tan \varphi = \frac{1}{\nu_0 T_2} = \frac{1}{\nu_0} \left(\frac{1}{T_c} + \nu_0^2 \tau_v \right) = \frac{\nu_0}{\beta p} (1 + p^2/p_m^2).$$

With increasing p the angle φ first decreases and then increases (Fig. 6 b) and assumes the minimum value

$$\tan \varphi(p_m) = \tan \varphi_{\min} = \frac{2\nu_0}{\beta p_m} = 2\sqrt{\frac{\alpha}{\beta}} \quad \left(p_m = \frac{\nu_0}{\sqrt{\alpha\beta}} \right)$$

at pressure $p_m \approx p_1$ (see Figs. 1 a, 3, and 5).

On the contrary, the time $T_2 = (\alpha p + \nu_0^2/\beta p)^{-1} = \alpha^{-1}(p + p_m^2/p)^{-1}$ attains maximum at $p = p_m$: $T_2(p_m) = T_{2,\max} = \sqrt{\gamma}/2\nu_0$ (Fig. 6 b). For $p \rightarrow 0$ and $p \rightarrow \infty$ the time T_2 tends to zero. However, the smaller p , the longer the time interval on which the polarization damping obeys the nonlinear exponential law, i.e., for small p the time T_2 no longer has the meaning of the effective relaxation time.

We note that φ and φ_{\min} can be determined only for sufficiently large $t > \tau_v(p)$ (when $L(t) \approx t/T_2 - \nu_0^2 \tau_v^2 y_1$). Thus, the characteristic values

$$t' = \tau_v(p_m) = \frac{1}{\nu_0 \sqrt{\gamma}}, \quad m' = \tau_v(p_m) \nu_0 \tan \varphi_{\min} = 2/\gamma$$

restrict the "dead zone" (which is hatched in Fig. 6 a) within which no extrema appear in the dependence of $\Delta\omega$, τ_{ph} , m_{ph} , and φ on p . It follows, for instance, that since the formation of the spectrum requires a damping $m \sim 1$, for the appearance of the Dicke dip the condition $m' < 1$ or $\gamma > 2$ must be fulfilled. Similarly, for the maximum of τ_{ph} it is necessary that $m > m'$ or $\gamma > 2/m$, and for the minimum of m_{ph} it is required that $\tau > \tau'$ or $\gamma > (\tau\nu_0)^{-2}$. These estimates agree well with the exact expressions for the thresholds of the appearance of extrema of the dephasing parameters (see below).

8. We now define the thresholds of the appearance of dips or peaks of the following parameters:

$\Delta\omega'_s$ for the integrated width of the noise spectrum of the spontaneous polarization;

$\Delta\omega'_a$ for the integrated width of the spectrum of active polarization excited by a monochromatic field or a wide-band noise field;

$\Delta\omega_\varepsilon$ for the width of the spectrum apex at the level $1 - \varepsilon$, $\varepsilon \ll 1$ (see (9));

τ_{ph} for the dephasing time;

m_{ph} for the dephasing decrement.

The spectrum widths are determined by the expressions (see [5, p. 167], and (9))

$$\Delta\omega'_s = \pi/\tau_1, \quad \Delta\omega'_a = 2\pi\tau_2/\tau_1^2, \quad \Delta\omega_\varepsilon = \sqrt{2\varepsilon\langle\tau^2\rangle^{-1}}, \quad (44)$$

where

$$\tau_1 = \int_0^\infty h(t) dt, \quad \tau_2 = \int_0^\infty h^2(t) dt, \quad \langle\tau^2\rangle = \frac{1}{\tau_1} \int_0^\infty h(t)t^2 dt. \quad (45)$$

For $h(t)$ we can write (see (1) and (8))

$$h(t) = \exp\left\{-\alpha pt - \nu_0^2 t^2 \sum_{n=0}^\infty \frac{(\beta pt)^n R_n}{(n+1)(n+2)}\right\}.$$

Consider the interval of low pressures. Up to within the terms of the first order with respect to p we have

$$h(t) \approx \exp\left\{-\frac{1}{2}\nu_0^2 t^2\right\} \cdot \left(1 - \alpha pt - \frac{1}{6}\nu_0^3 \beta R_1 t^3 p + \dots\right). \quad (46)$$

Substituting (46) into (45) and (44) we obtain for the interval of low pressures the expressions

$$\Delta\omega'_s = \sqrt{2\pi} \left[\nu_0 + \frac{\alpha p}{\sqrt{\pi/2}} \left(1 + \frac{1}{3} R_1 \gamma\right) \right] \quad \left(\gamma > \frac{3}{|R_1|}\right),$$

$$\Delta\omega'_a = 2\sqrt{\pi} \left[\nu_0 + \alpha p \frac{2(\sqrt{2}-1)}{\pi} \left(1 + \frac{1}{3} R_1 \gamma \frac{2\sqrt{2}-1}{2(\sqrt{2}-1)}\right) \right]$$

$$\left(\gamma > \frac{3}{|R_1|} \frac{2\sqrt{2}-2}{2\sqrt{2}-1} \approx \frac{3}{|R_1|} \cdot 0.45\right),$$

$$\Delta\omega_\varepsilon = \sqrt{2\varepsilon} \left[\nu_0 + \frac{\alpha p}{\sqrt{2\pi}} \left(1 + \frac{1}{6} R_1 \gamma\right) \right] \quad \left(\gamma > \frac{3}{|R_1|} \cdot 2\right),$$

$$\tau_{ph} = \tau_0 - \frac{\alpha p}{\nu_0^2} \left(1 + \frac{1}{3} m \gamma R_1\right) \quad \left(\gamma > \frac{3}{|R_1|} \frac{1}{m}\right), \quad (47)$$

$$m_{ph} = m_{ph,0} + \left(1 + \frac{1}{6} \gamma R_1 \nu_0^2 \tau^2\right) \alpha p \tau \quad \left(\gamma > \frac{3}{|R_1|} \frac{2}{\nu_0^2 \tau^2}\right), \quad (48)$$

where $\alpha p = T_c^{-1}$ and $\gamma = \beta/\alpha = T_c/\tau_0$ (in the parentheses on the right the conditions for the appearance of the characteristic extrema are indicated).

These results show that for $\Delta\omega_\varepsilon$ the threshold of the appearance of the Dicke dip turns out to be even higher than for the integrated bands $\Delta\omega'_s$ and $\Delta\omega'_a$ corresponding to approximately $\varepsilon = 0.5$. From formulas (47) and (48) it is also seen that in the nonstationary spectroscopy the threshold value of γ can be arbitrarily decreased by choosing sufficiently large m and τ . Thus, in principle, the peak of the function $\tau_{ph}(p)$ and the dip of the function $m_{ph}(p)$ can be observed in any substance.

9. As was already noted in Section 5 (see formula (32) and its discussion) the case $R(x) = R(x^2)$ requires a special consideration. It turns out that in this situation the curves $\Delta\omega(p)$, $\tau_{ph}(p)$, and $m_{ph}(p)$ have additional weak extrema in the interval of low pressures (see the dashed curves in Figs. 1, 4, and 5) [5].

We note that the dependence of the correlation coefficient on τ^2 and not on τ is quite possible from the standpoint of the theory of random processes [8]. Moreover, we can assert that for every real random process the function $R(\tau)$ must have a rounded apex, that is, there must be $R_1 = 0$.

For $R(x) = R(x^2)$ we have (see (13) and (14))

$$R(x) = \sum_{n=0}^{\infty} R_{2n} x^{2n},$$

$$F(x) = \int_0^x (x-y)R(y) dy = x^2 \sum_{n=0}^{\infty} R_{2n} \frac{x^{2n}}{(2n+1)(2n+2)}.$$

As an example, we consider the appearance of an additional extremum (maximum) of the dephasing decrement. Expression (35) is now written as

$$n_{\text{ph}}(u) = u + 2n_0 F(u)u^{-2} = u + 2n_0 \sum_{s=0}^{\infty} \frac{R_{2s} u^{2s}}{(2s+1)(2s+2)}. \quad (49)$$

We assume (in what follows this will be confirmed) that the desired maximum lies in the interval of small p . Keeping the terms of the order not higher than the second with respect to $u = \beta p \tau$ in formula (49) we obtain

$$n_{\text{ph}}(u) = n_0 + u - \frac{1}{6} n_0 |R_2| u^2, \quad (50)$$

whence follows

$$n_{\text{ph}, \text{max}} = n(u_2) = n_0 + \frac{1}{2} u_2, \quad u_2 = \frac{3}{n_0 |R_2|}, \quad (51)$$

or, on passing to m_{ph} and p ,

$$m_{\text{ph}, \text{max}} = m_{\text{ph}, 0} + \frac{3}{|R_2|(\gamma \nu_0 \tau)^2}, \quad p_2 = \frac{6\alpha}{|R_2|(\gamma \nu_0 \tau)^2} \quad \left(m_{\text{ph}, 0} = \frac{1}{2} \nu_0^2 \tau^2 \right).$$

It is natural to compare the pressure p_2 with the pressure p_1 for which the functions $m_{\text{ph}}(p)$ and $n_{\text{ph}}(u)$ have a minimum analogous to the Dicke dip. However, in the general case neither the conditions for the appearance of the dip nor the value of p_1 are known. Therefore we resort to the dephasing model (32). In this case (49) takes the closed form

$$n_{\text{ph}}(u) = u + 2n_0 \frac{\sqrt{1+u^2} - 1}{u^2}. \quad (52)$$

If curve (52) has a minimum at $u = u_1$ and a positive derivative at $u = 0$ (see (50)), then it must intersect the initial level n_0 at at least three points:

$$u = 0, \quad u = u'_0 < u_1, \quad u = u_0 > u_1 \quad (u_1 = p_1 \beta \tau).$$

Let us estimate the position of these points. Setting $n_{\text{ph}} = n_0$ in (52) we obtain, after some transformations, the cubic equation $v(1-v^2) = \varepsilon$, $v = u/n_0$, $\varepsilon = 4/n_0^2$. It is equivalent to the equation $w^3 + pw + q = 0$ ($w = v - 2/3$, $p = -1/3$, and $q = 2/27 - \varepsilon$) with the discriminant $D = (p/3)^3 + (q/2)^2 = 4\varepsilon(\varepsilon - 1/(4 \times 27))$.

As is known, to the real roots of a cubic equation there corresponds $D < 0$. Consequently, in the case under consideration there must be

$$\varepsilon < 1/(4 \times 27), \quad (54)$$

that is $n_0 > 12\sqrt{3}$.

Since, according to (54), the parameter ε can be assumed to be small ($\varepsilon \ll 1$), the above equation for v yields $v'_\varepsilon \approx \varepsilon$, $v_0 \approx 1 - \sqrt{\varepsilon} \gg v'_0$, and

$$u'_0 \approx 4/n_0, \quad u \approx n_0 - 2 \gg u'_0. \quad (55)$$

We have shown that the maximum of the function $n_{\text{ph}}(u)$ corresponds to small values of u (the "width" of the maximum is $u'_0 = 4/n_0 \ll 1$). This justifies the earlier estimates (51), which in the case of (52) assume the form

$$n_{\text{ph}, \text{max}} = n_0 + 1/n_0, \quad u_2 = 2/n_0.$$

However, this is a weak maximum:

$$n_{ph, \max}/n_0 - 1 = 1/n_0^2 \lesssim 2.6 \cdot 10^{-3},$$

and it seems to be difficult to register it experimentally.

10. The main results of the presented theory — the description of the signal observed in the non-stationary active spectroscopy and the dependence of the dephasing time on pressure — were confirmed experimentally in [4]. In this case in the installation (Fig. 7) use was made of short (picosecond) optical pulses at frequencies ω_1 and $\omega_2 = \omega_1 + \omega_0$ (where ω_0 is the frequency of molecular oscillations) with a delay τ at the test frequency ω_{p1} . The output signal proportional to $h(t)$ was observed at the anti-Stokes frequency $\omega_{a1} = \omega_{p1} + \omega_0$. We shall call it channel 1 of the system.

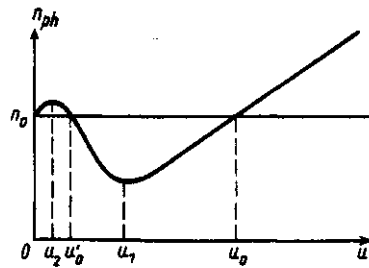


Fig. 7

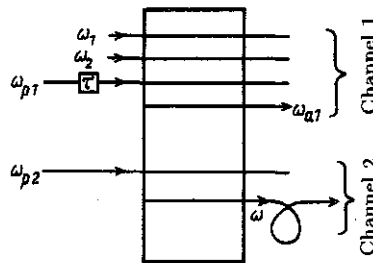


Fig. 8

It appears interesting to supplement the installation with channel 2, without any violation of the operation of channel 1, by transmitting one more test wave through the substance, namely *continuous* radiation at a second test frequency ω_{p2} (Fig. 8). In this case a long output pulse with envelope proportional to $h(t)$ will be formed at, for instance, the second anti-Stokes or Stokes frequency $\omega = \omega_{p2} \pm \omega_0$, whose form will repeat that of the pulse of damped molecular oscillations. If this pulse is then transmitted through a lightguide filled with a dispersive medium (e.g., through an optical fiber), then, on passing a sufficiently long distance, the pulse undergoes Fourier's transformation and turns into a "spectron" — a pulse whose envelope repeats the frequency spectrum of the primary pulse [3, 5].

As a result, it becomes possible to observe in a single installation the function $h(t)$ in both the strobed form (in channel 1: $h(t)$, $\tau = \tau_1, \tau_2, \dots$) and the "natural" form (the beginning of channel 2) together with the time-base of its spectrum (the end of channel 2). Consequently, in such a system it is possible to measure simultaneously the dephasing time τ_{ph} , the decrement m_{ph} and the spectrum width $\Delta\omega$, and to observe the spectrum itself at different pressures — all this on the basis of *nonstationary* spectroscopy [6].

The latter possibility is related to one more specific property of the suggested channel 2, namely to measure the spectrum we need only use a single laser shot.

In conclusion we note that channel 2 can also operate when channel 1 is partly switched off, namely when the pulse generation at the first test frequency ω_{p1} and the delay line τ are switched off.

The dispersion lengths $l_n = \tau^n/k_n$ ($k_n = \partial^n k/\partial \omega^n \sim 2 \times 10^3$ (fs)ⁿ/cm in the wave band $\lambda \sim 1 \mu\text{m}$) correspond to a pulse with duration τ , and the condition of the formation of an undistorted spectrum on the length l can be written as $l_2 \ll l \ll l_3$. Estimating τ as $T_{2,\text{max}} = T_2(p_m) = \sqrt{\gamma}/2\nu_0$ or as $\tau_{\text{ph,max}} = \frac{M+1}{\nu_0\sqrt{\gamma}} \approx \frac{M}{\nu_0\sqrt{\gamma}} = \frac{\sqrt{\gamma}}{2\nu_0} \frac{2m|R_1|}{3}$ we obtain in the case of gaseous hydrogen ($\gamma = 64$, $\nu_0 = 3 \times 10^9 \text{ s}^{-1}$) the values $\tau \simeq 1 \text{ ns}$, and $l_2 \simeq 5 \times 10^8 \text{ cm}$, $l_3 \simeq 5 \times 10^{14} \text{ cm}$. Hence, the effective length of the optical fiber must be of the order of $l > 5 \times 10^3 \text{ km}$.

REFERENCES

1. S. A. Akhmanov and N. I. Koroteev, *Methods of Nonlinear Optics in Light Scattering Spectroscopy* (in Russian), Moscow, 1981.
2. W. Demtröder, *Laser Spectroscopy. Basic Concepts and Instrumentation*, Berlin, Heidelberg, 1982.
3. Yu. E. D'yakov, *Pis'ma v ZhETF*, vol. 37, no. 1, p. 14, 1983.
4. Yu. E. D'yakov, S. A. Krikunov, S. A. Magnitskii, *et al.*, *ZhETF*, vol. 84, no. 6, p. 2013, 1983.
5. Yu. E. D'yakov and S. Yu. Nikitin, *Problems in Statistical Radiophysics and Optics* (in Russian), Moscow, 1985.
6. Yu. E. D'yakov, *Lasers in National Economy (Proc. of the RSFSR "Znanie" Society Seminar)* (in Russian), p. 99, Moscow, 1991.
7. S. G. Rautian and I. I. Sobel'man, *Uspekhi Fiz. Nauk.*, vol. 90, no. 2, p. 209, 1966.
8. S. A. Akhmanov, Yu. E. D'yakov, and A. S. Chirkin, *Introduction to Statistical Radiophysics and Optics* (in Russian), Moscow, 1981.

20 September 1991

Department of General Physics
and Wave Processes